R 641

Technical Report

SEA-ICE BEARING STRENGTH IN ANTARCTICA—AIRCRAFT LOAD CURVES FOR MCMURDO ICE RUNWAY

September 1969

Sponsored by

NAVAL FACILITIES ENGINEERING COMMAND

U. S. NAVAL CIVIL ENGINEERING LABORATORY

Port Hueneme, California

41

CONTENTS

BLANK PAGE

INTRODUCTION

Adequate airfields can be economically constructed and maintained on annual sea-ice fields overlying bodies of water that are sufficiently deep to prevent grounding. An example is the airfield at McMurdo, Antarctica, which has been used each season since Deep Freeze I (1955-56). Research continues to increase our understanding of the properties affecting the mass behavior of the ice sheet; it is therefore important to periodically update operating criteria.

This report develops a new series of load-versus-ice-thickness curves for C-121, C-130, C-124, C-141, and C-5 aircraft. They are intended to supersede the curves presented in Reference 1, which are currently used as operational guidance criteria.

Development of operational criteria for aircraft traffic on a floating ice sheet from analysis of the structural behavior for the various aircraft load patterns involves bringing together three fundamentals: (1) knowledge of those mechanical properties critical to the solution, (2) theory that will adequately describe the load condition, and (3) a definition of the failure criteria by which an appropriate safety factor can be included in the solution. Any deficiency in this information must be replaced by an engineering judgment.

The aircraft load curves developed in this report have eliminated many of the empirical solution techniques used previously.[1] This has been accomplished by application of the general classic plate theories for predicting the elastic behavior.

CHARACTERISTICS AND STRENGTH PROPERTIES OF MCMURDO SEA ICE

Temperature, salinity, and age each affect the bearing strength of an ice sheet. The total combined effect of these parameters generally results in an ice plate with strength characteristics that are nonhomogeneous in the vertical dimension. It is not now possible to separate the three parameters in terms of their individual contribution to strength, and then recombine them to define a new strength–time condition.

Fortunately, for a short-term operation such as the period between October to February, when aircraft land on the McMurdo annual sea ice, the only variable in strength analysis is temperature. During this short period there is no appreciable change in ice properties from salinity variation and aging. Salinity profiles of the ice sheet taken during the operational period were reasonably constant. The salinity profile from year to year also varied little because the sea-ice runway for the past several years has been located on annual ice.

Although the strength–temperature relationship of ice is fairly well defined, mathematical structural theory for analyzing a plate with a temperature-gradient condition is deficient. To permit the application of standard plate theories for the analysis, the effective flexural strength during the operational period, when there was a temperature gradient in the ice sheet, was determined by full-scale in-situ beam tests of the ice. Tests were also performed at the end of the warm-up season, late January to early February, when the ice sheet was essentially isothermal. These tests provided a range of flexural strength data that corresponds with the temperature-gradient profiles (Figure 1). These profiles indicate the trend of warming for the ice sheet during the operational period. To further simplify the temperature–flexural strength relationship for field application, the temperature at the 24-inch stratum was selected as the correlative point. Investigation has shown that temperature measurements at this depth in the ice sheet are reasonably insensitive to the daily fluctuation of the air temperature, provide a clear record of the seasonal temperature trend, and are easy to monitor. The curve in Figure 2 represents the expected seasonal temperature at the 24-inch depth based on a three- to four-season record. Superimposed on the same temperature curve in Figure 3 are the allowable flexural strengths as determined from in-situ beam tests. The allowable flexural strength indicated for each of four time–temperature periods (discussed below) is the result of reducing the failure strength by the percentage indicated at the bottom of Figure 3. This difference between allowable strength and failure strength represents a safety factor incorporated in the solution of the aircraft load curves developed later. For convenience and simplification of the analysis, the allowable flexural strength has been distributed along the temperature curve (Figure 3) as a step function rather than as a continuous temperature-dependent function; the latter probably represents the true condition. The indicated safety factor applies only to the numerical value given for the allowable stress, which is the approximate midperiod strength for periods 1, 2, and 3; and the extreme right-hand side of period 4.

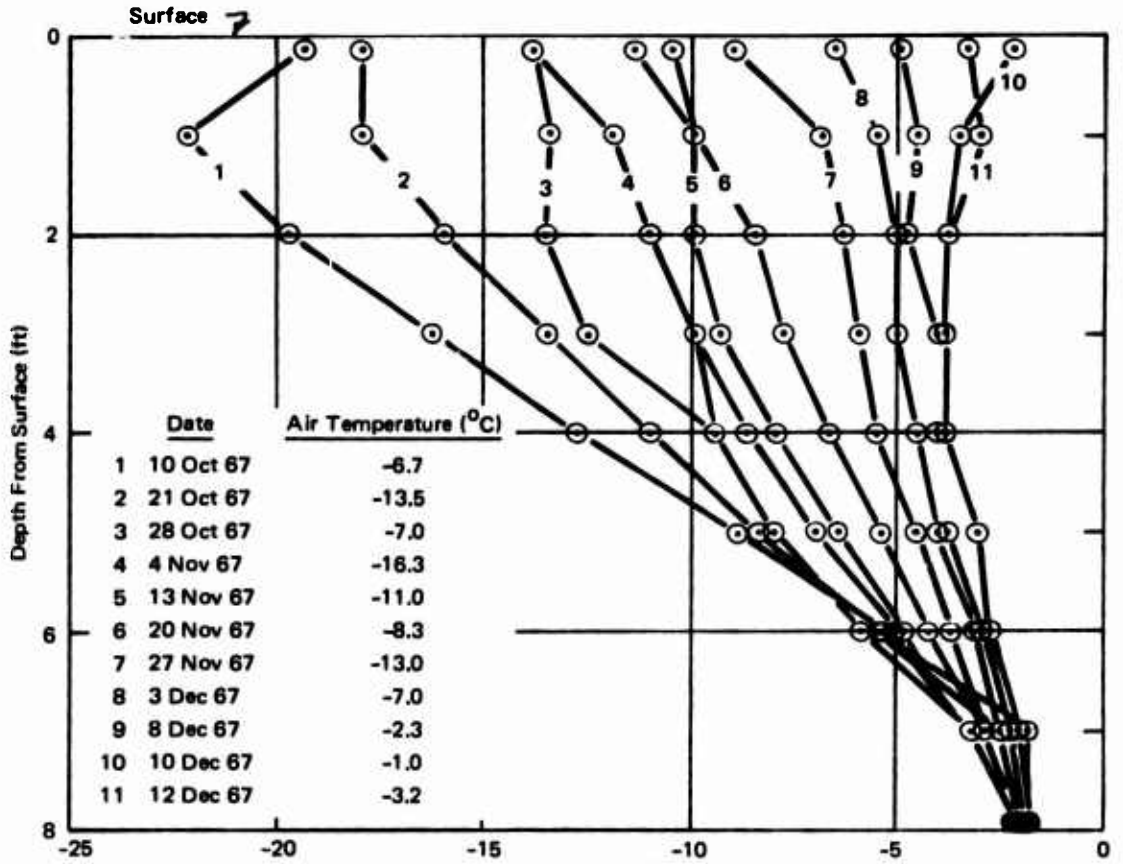

Figure 1. Temperature of annual sea-ice sheet, McMurdo (near shelf end of runway, no snow cover).

Division of the ice condition during the runway use period into four time—temperature periods logically reflects the effect of progressive warming and internal melting. In periods 1 and 2 (Figure 3), most of the strength deterioration results from steepening of the temperature gradient or general warm-up of the ice sheet. In period 4, the strength deterioration is due to a stagnation period of an isothermal gradient at near-melting temperature. Period 3 includes both the effect of the later phase of the general ice-sheet warm-up and the beginning of the internal melting phase.

The elastic modulus property of the ice, which is also needed in the elastic analysis of bearing strength, can be expected to behave in a manner similar to the flexural strength. Since no local data is available for this property, it is necessary to select published values primarily of arctic origin. The literature provides values for this property of sea ice determined both by static and dynamic experimental methods. Dynamic modulus values, obtained seismologically (the predominant test method), are appreciably

higher than those obtained by static or deflection measurement methods. Though both test methods have their recognized deficiencies, the dynamic values are more widely accepted as representing the ice-sheet behavior. The elastic modulus values selected with reference to the ice temperature periods of Figure 3 are given in the table below, together with associated allowable flexural-strength values.

Period	Elastic Modulus (psi x 10^5)	Flexure Strength (psi)
1	7	80
2	6	70
3	4	55
4	2.9	35

The influence of elastic modulus values on the numerical results of the analysis will be discussed later. In addition to the flexural-strength and elastic-modulus properties, Poisson's ratio (the ratio between transverse and longitudinal strain) is needed for analyzing the bearing strength. A value for Poisson's ratio of 0.3 was assigned on the basis of reports of experiments that indicated a variation from 0.29 to 0.33.

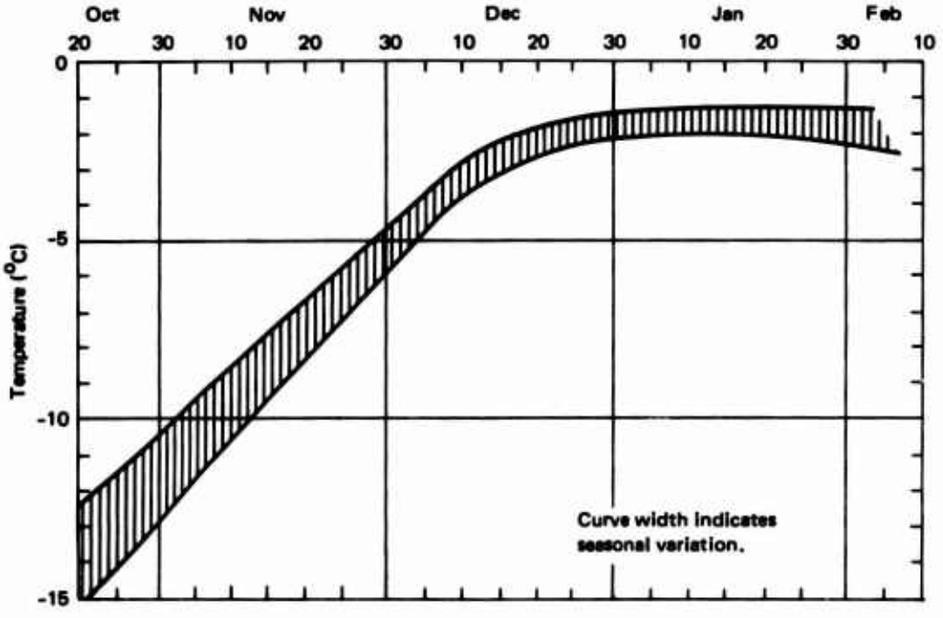

Figure 2. Temperature of McMurdo annual sea ice at 24-inch depth (based on records for at least three seasons).

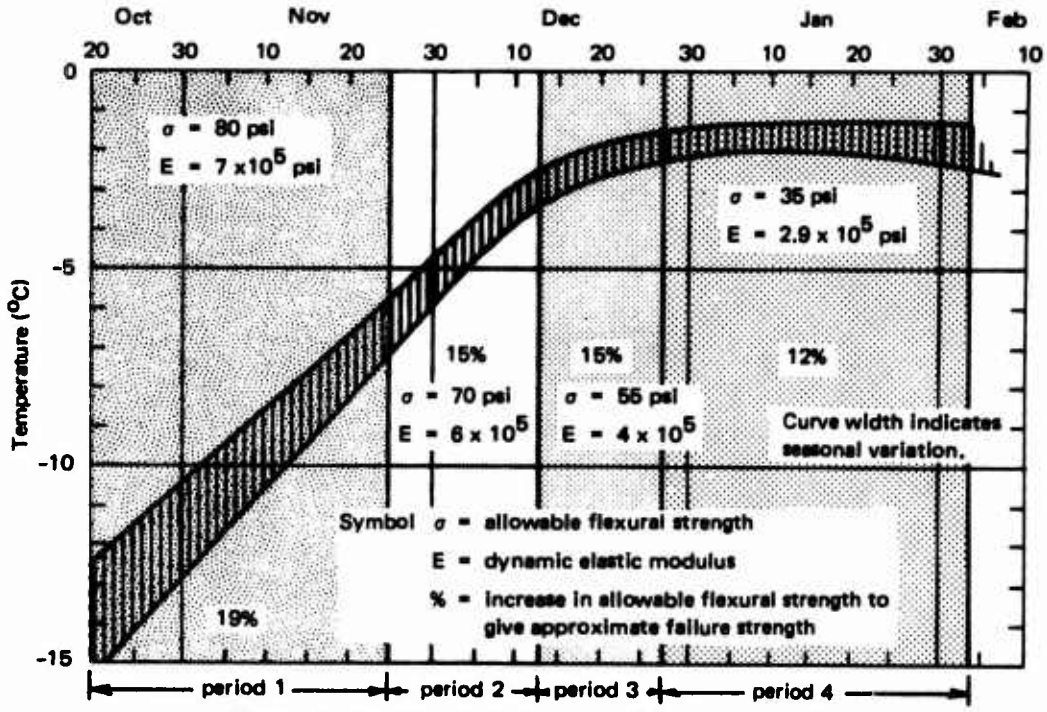

Figure 3. Ice-sheet strength versus 24-inch temperature.

DISCUSSION OF ANALYTICAL METHOD

A floating annual ice sheet of infinite size can be analyzed by elastic theory as a plate resting on an elastic foundation. The ice sheet has flexural rigidity; as it deflects, there is a restoring force due to the water pressure which is proportional to the deflection. Simplifying assumptions in the criteria used to develop the aircraft load curves were: (1) the ice behaves as an isotropic medium, (2) its relaxation characteristics are outside the domain of the loading times, and (3) the moving surface loads do not create resonance wave conditions in the plate.

The solution was based on superimposing the load effect of the adjacent landing gear for a particular aircraft configuration on the results produced by one main gear positioned over the zero coordinates of a rectangular coordinate system (Figure 4). The load carried by each gear is considered uniformly distributed over a circular area (Figures 5 through 9). Using the equation developed by Westergaard,[2] the radius of the load circle was adjusted to relate the load circle radius to the thickness of the ice plate for all values of the radius less than 1.724 times the sheet thickness.

$$b_1 = \sqrt{1.6\,a^2 + h^2} - 0.675\,h \qquad (1)$$

where b_1 = adjusted radius of load circle (in.)

a = original radius of load circle (in.)

h = thickness of ice sheet (in.)

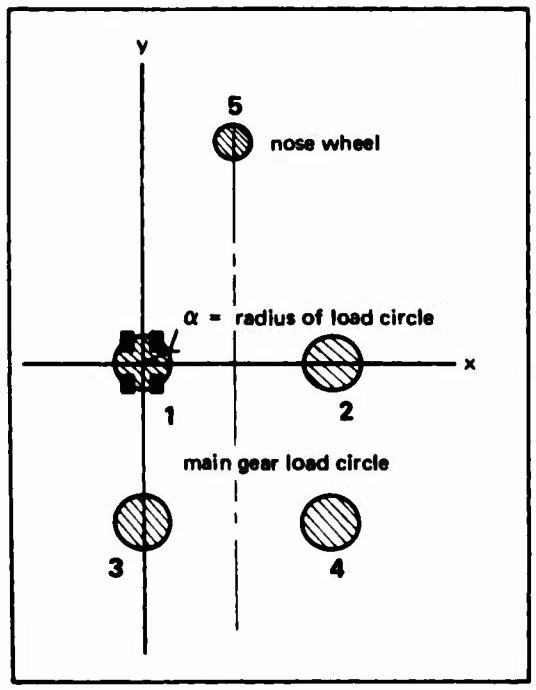

Figure 4. Typical position of aircraft landing gear on rectangular coordinate system for superimposing stresses and deflections.

For the complete mathematical formulation of the problem, together with an outline of the computer solution, see Appendix A.

The fundamental differential equations formulating the solution were taken from "Theory of Plates and Shells," by Timoshenko and Woinowsky-Krieger[3] and Wyman's publication, "Deflection of an Infinite Plate."[4] Wyman presented formula referenced to Timoshenko's work, giving stress and deflection formula for a constant density circular load on an infinite ice sheet supported by water. From this, a mathematical solution was developed for the superposition effect of the gear configuration for C-121, C-124, C-130, C-141, and C-5 aircraft.

To begin the analysis for developing the aircraft load curves, the effect of one of the aircraft's main landing gear placed at the zero coordinate point was analyzed for moment and stress, using the basic equations presented by Wyman.[4] For the left-hand side of the equations to follow, the subscript **r** represents radial direction, and **t** represents tangential direction for moment and stress condition. The expressions given in Wyman's report for bending moments are:

$$M_r = -D\left[\frac{d^2w}{dr^2} + \frac{\mu}{r}\left(\frac{dw}{dr}\right)\right]$$

$$M_t = -D\left[\frac{1}{r}\left(\frac{dw}{dr}\right) + \mu\frac{d^2w}{dr^2}\right]$$

where **r** = radius from load center*

w = deflection of middle plane of the plate*

* From right-hand side of equation.

For tensile stress the expressions are:

$$(\sigma_r)_{max} = -6 \frac{(M_r)_{max}}{h^2}$$

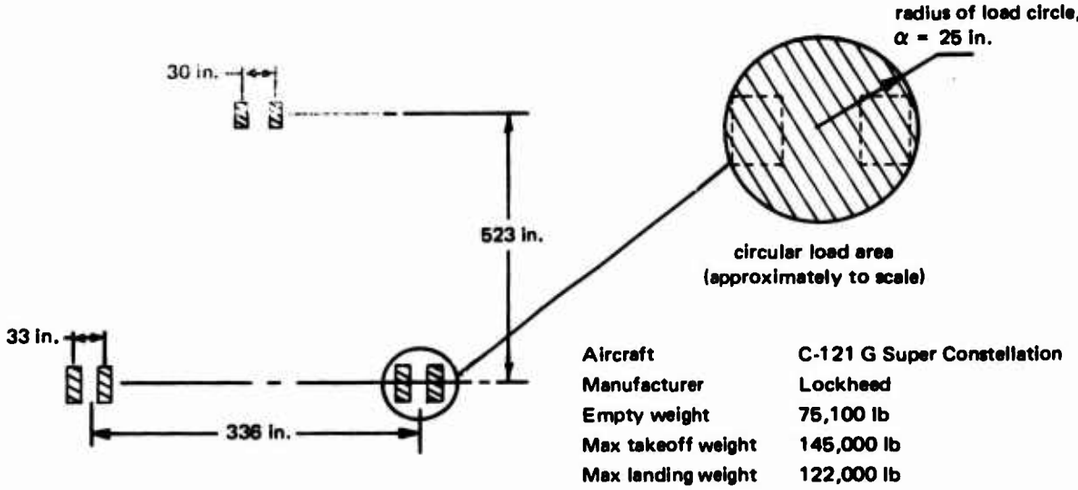

Aircraft	C-121 G Super Constellation
Manufacturer	Lockheed
Empty weight	75,100 lb
Max takeoff weight	145,000 lb
Max landing weight	122,000 lb
Weight on main gear	95.5%
Max static wheel load	34,600 lb
Tire pressure	130 psi
Tire contact area	226 in.^{2}
Footprint width	14.3 in.

Figure 5. Aircraft characteristics for the C-121.

For the assumption that maximum moment occurs at $r = 0$ (r = radial distance from zero coordinates), then $M_r = M_t$. The stress equation when the total load, P, is assumed distributed over the circular load areas of the ice plate supported on an elastic foundation is represented by:

$$(\sigma_r)_{max} = \frac{3P\,b\,D(1+\mu)\,kei'b}{\pi a^2 K h^2 \ell^2} \qquad (2)$$

where $\sigma_r = \sigma_t$ = max, stress

P = total load distributed over circular load area

μ = Poisson's ratio (assumed in this solution to have value 0.3)

$'$ = derivative of the modified Bessel function **kei b**, where $b = a/\ell$, a = radius of the load circle, and ℓ = radius of relative stiffness ($\ell^4 = D/K$)

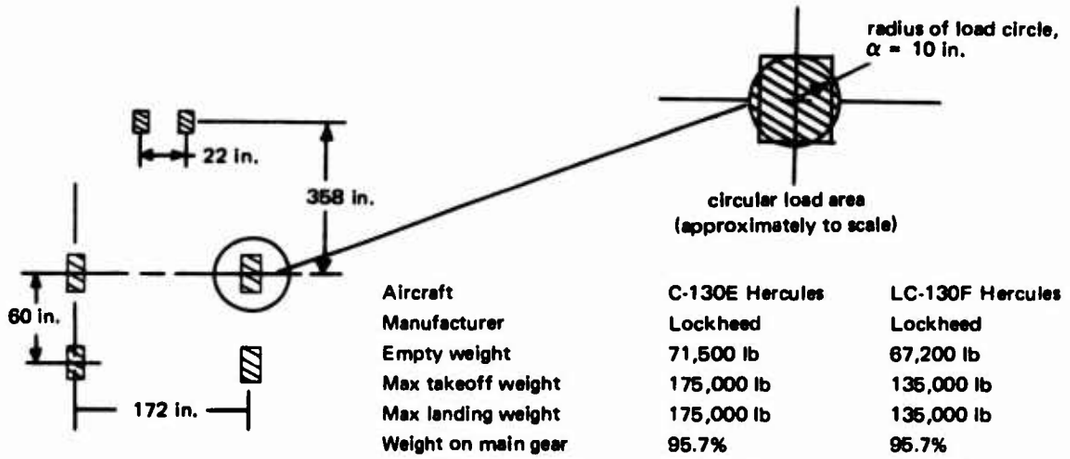

Aircraft	C-130E Hercules	LC-130F Hercules
Manufacturer	Lockheed	Lockheed
Empty weight	71,500 lb	67,200 lb
Max takeoff weight	175,000 lb	135,000 lb
Max landing weight	175,000 lb	135,000 lb
Weight on main gear	95.7%	95.7%
Max static wheel load	41,900 lb	32,300 lb
Tire pressure	95 psi	95 psi*
Tire contact area	400 $in.^2$	340 $in.^2$
Footprint width	18.3 in.	—

* Assumed

Figure 6. Aircraft characteristics for the C-130.

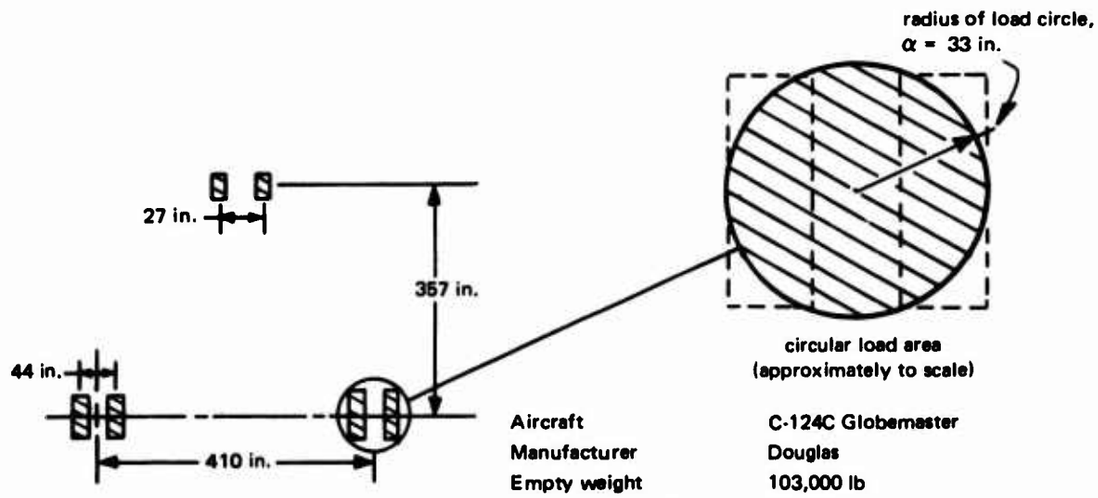

Aircraft	C-124C Globemaster
Manufacturer	Douglas
Empty weight	103,000 lb
Max takeoff weight	216,400 lb
Max landing weight	194,500 lb
Weight on main gear	93.4%
Max static wheel load	50,600 lb
Tire pressure	79 psi
Tire contact area	640 $in.^2$
Footprint width	22.1 in.

Figure 7. Aircraft characteristics for the C-124.

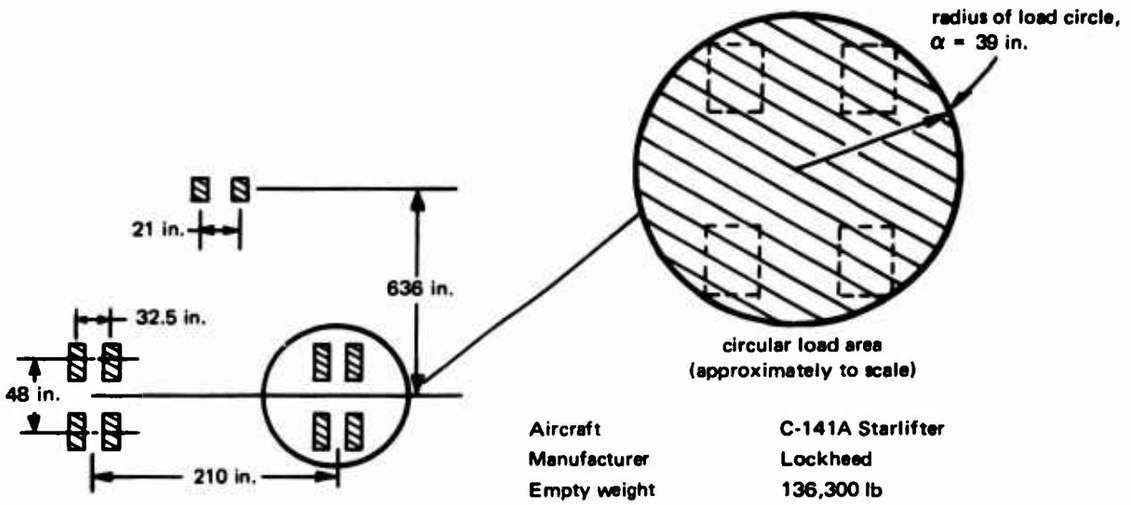

Aircraft	C-141A Starlifter
Manufacturer	Lockheed
Empty weight	136,300 lb
Max takeoff weight	316,100 lb
Max landing weight	316,100 lb
Weight on main gear	94.4%
Max static wheel load	37,400 lb
Tire pressure	180 psi
Tire contact area	208 in.^{2}
Footprint width	12.6 in.

Figure 8. Aircraft characteristics for the C-141.

K = foundation modulus (for this solution, the density of water = 0.037 lb/in.^{3})

D = flexural rigidity of the plate, derived from equation $D = Eh^3/12(1 - \mu^2)$, where E = elastic modulus of plate and h = thickness of plate

The superposition of the components of stress for the remaining aircraft landing gear onto the initial stress condition produced by the gear at the zero coordinate point was accomplished by a summation of partial derivatives of the bending effect relative to the coordinate position of the particular gear. If we let $v_i = w_i/P$, where w_i = plate deflection produced by any one of the off-zero coordinate landing gear, then

$$\frac{\partial^2 v}{\partial x^2} = \sum_i \frac{\partial^2 v_i}{\partial x^2}, \quad \frac{\partial^2 v}{\partial y^2} = \sum_i \frac{\partial^2 v_i}{\partial y^2}, \quad \frac{\partial^2 v}{\partial x\,\partial y} = \sum_i \frac{\partial^2 v_i}{\partial x\,\partial y}$$

The total deflection of the ice plate from loading by the aircraft was calculated by the same general technique used for stress calculation.

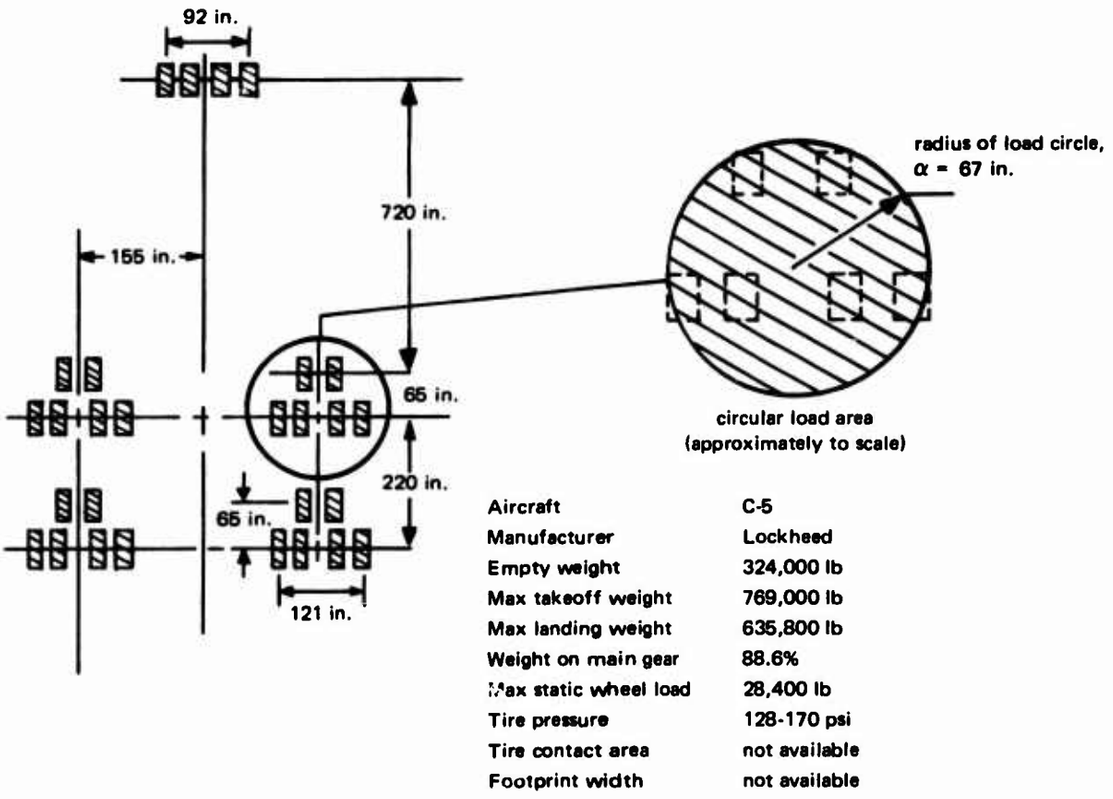

Figure 9. Aircraft characteristics for the C-5.

Starting with the basic deflection equation[3] for the r = 0 condition for the gear at the zero coordinate location, the deflection is given by

$$w_{max} = \frac{P[1 + b\,ker'(b)]}{\pi r^2 K} \tag{3}$$

The superimposed deflection resulting from each adjacent gear is given by the general equation

$$w = \frac{Pb}{\pi r^2 K}\left[ber'(b)\,ker\left(\frac{r}{\ell}\right) - bei'(b)\,kei\left(\frac{r}{\ell}\right)\right] \tag{4}$$

where r = radial distance between the zero coordinate gear and the coordinate position of the gear being analyzed

The total deflection is summed by method of partial derivatives.

DISCUSSION OF ANALYTICAL RESULTS

The aircraft load curves presented in this report are the results of a more comprehensive treatment of the problem than was used for the load curves developed in Reference 1, which are currently a part of the Navy Deep Freeze Operation Orders.* However, the differences between present operating criteria and operating criteria suggested by the newly developed curves are not great. The new criteria establish a better relationship between the flexural-strength property and the transient 24-inch-depth temperature curve of the ice sheet, and replace empirical solution techniques with a solution based on close adherence to elastic plate theory.

The in-situ beam flexural-strength studies conducted at McMurdo assure reasonably accurate breaking strength data for ice at both the high- and low-strength ends of the operating season in addition to some data on the intermediate condition. Using this data, it was possible to translate the operating season ice condition into four criteria periods, each representable by a single load curve, as opposed to the three curve periods in the original solution.[1] The allowable flexural-strength values used for the analysis are a reduced value of flexural strength at failure by an amount ranging from 12% to 19% as indicated in Figure 3. As can be observed from general Equation 2, the allowable value for flexural strength has considerable effect on the solution, since it enters the equation as a first-order term in the numerator.

The flexural rigidity of a material is determined by the elastic modulus of the material and enters into the theoretical solution as a parameter for deriving the bending moment. Like flexural strength, the elastic modulus property is temperature dependent. For this analysis, as in the preceding work,[1] it was necessary to substitute literature-reported modulus values for nonexistent antarctic data. A case study was made to determine the effect of varying modulus value on the calculated load capability (Figure 10). From this case study, it is apparent that the influence of the elastic modulus property is not appreciable; e.g., a 100% error in the assigned value would alter the calculated load capacity of the ice sheet by less than 10%. The error involved in translating arctic-obtained data to antarctic ice conditions would probably not exceed the 10% effect on the calculated load capacity. Support for this assumption is based on: (1) the consistency in dynamic value of the elastic modulus property found in the literature for a wide variation of arctic locales, (2) the fairly explicit definition of the property as related to both temperature and salinity, and (3) the relatively narrow band of modulus variation (approximately 2.9×10^5 to 10×10^5 lb/in.^{2}) for a wide range of temperature and salinity.

* Task Force 43 Operation Order No. 1-67, Operation Deep Freeze 68.

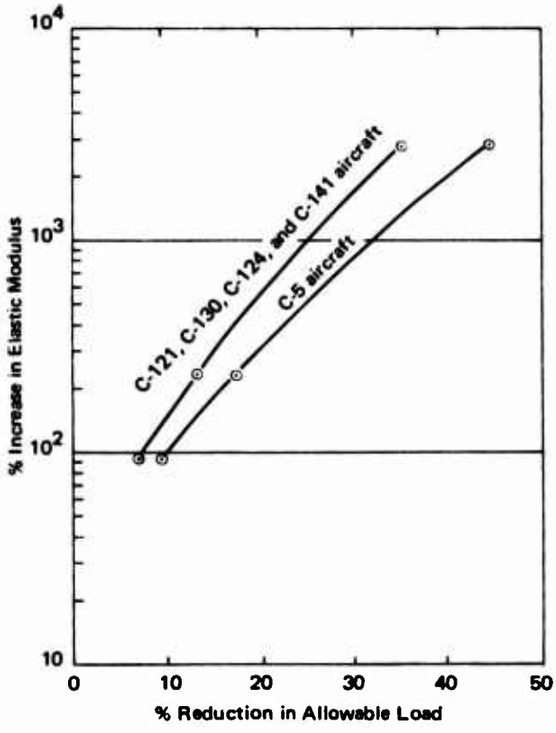

Figure 10. Effect on allowable load resulting from constant stress (35 psi) and varying elastic modulus.

From Equation 2, it can be observed that both the numerator and denominator of the equation have terms containing the parametric effect of the elastic modulus property, which accounts for the appreciably smaller influence it has on the solution than is the case for the flexural-strength property.

Each aircraft establishes an individual load-versus-ice-thickness curve as a result of its particular landing gear configuration. For this analysis the stress condition of the ice sheet results from the local stress produced by the gear positioned over the zero coordinate plus the superimposed stresses from the other load areas corresponding to the total landing gear configuration. In general, it was found that the zero coordinate gear produces more than 50% of the total stress caused by the aircraft. The load curves developed for each aircraft are shown in Figure 11. While the C-5 has a requirement distinctly different from the other aircraft, the close grouping of the C-121, C-130, C-124, and C-141 load curves justifies a single curve representation to simplify use. The simplified load curves for operational use are shown in Figure 12. Each of these curves (Figure 11) represents the centroid of the grouping for the C-121, C-130, and C-141 aircraft. Thus, they are conservative in representing the required thickness for the C-124 aircraft. Sacrifice in optimum operating criteria for the C-124 in favor of the other aircraft is considered justified because of its infrequent present-day use in sea-ice operations.

By comparing this set of curves with those in Reference 1, it can be seen that an attempt has been made to more finitely associate the operating criteria with narrower ice temperature ranges. The result is that curve 3 in Figure A-1 of Reference 1 has been replaced by two curves 3 and 4 to cover essentially the same late warm season operation period. Curve 1 is identical to the previous curve 1 regarding the load-versus-thickness requirement except for an extended use period. Curve 2 of the new set both reduces the thickness requirement and extends the use period.

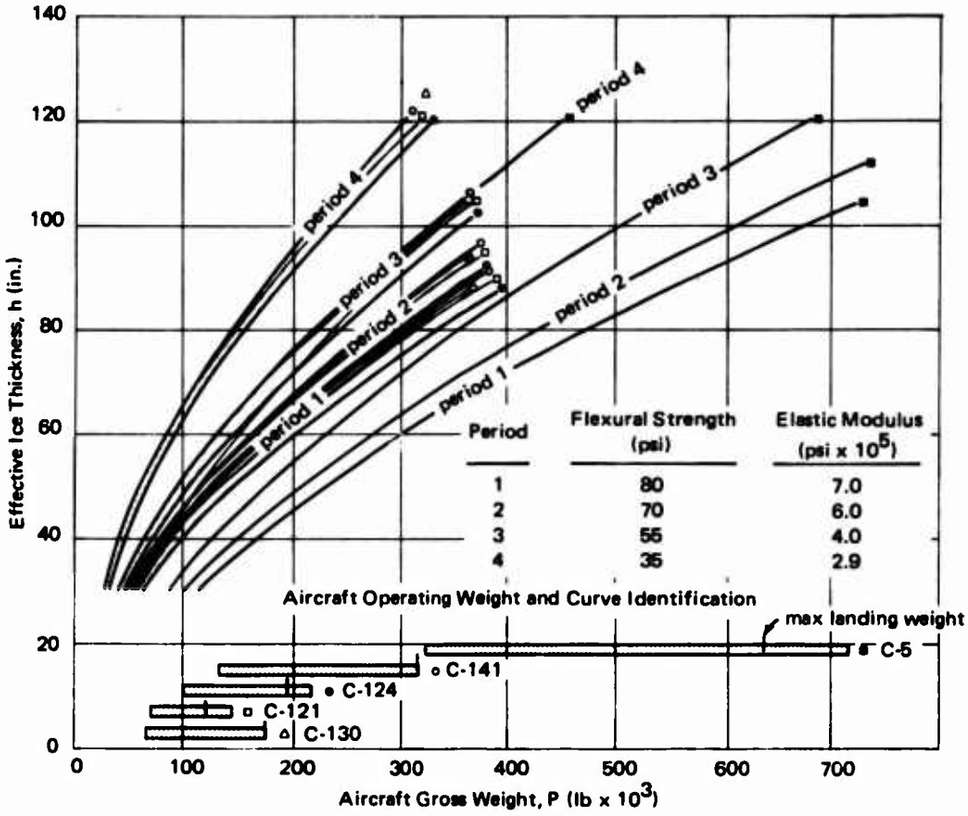

Figure 11. Load curves showing effect of landing gear configuration.

The load curves for operating the C-5 aircraft from ice runways are given in Figure 13. The runway thickness requirement for this aircraft is appreciably less than that for the other aircraft due to the load distribution of its landing gear.

The deflection of the ice sheet for the various aircraft is given in Figures 14 through 16. The curves represent the maximum deflection caused by the superimposed effect of the landing gear for the maximum landing weight of the aircraft.

SUMMARY

This study is a continuation of effort to apply current knowledge of the properties of ice and current analytical techniques in redefining aircraft operation criteria for sea-ice airfields. The analysis has been limited to the elastic response of the ice plate, and as appropriate throughout the report, comparison is made with the previous solution.[1]

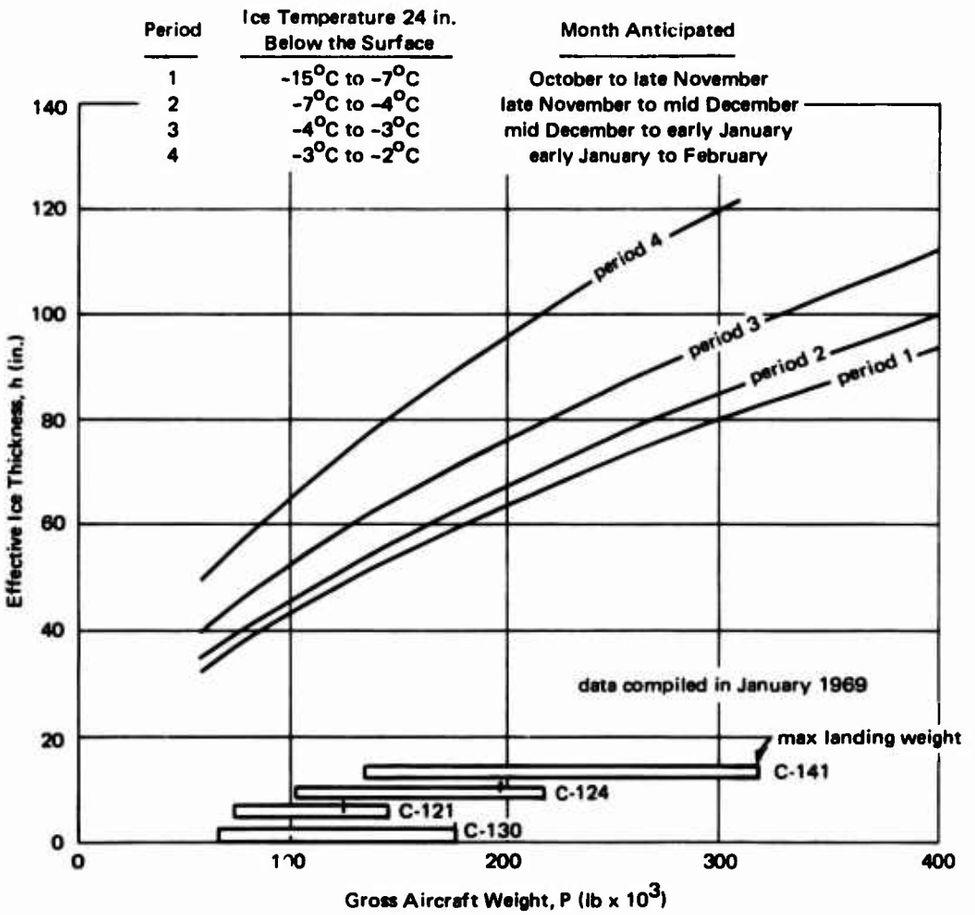

Figure 12. Load-versus-thickness requirements for C-130, C-121, C-124, and C-141 aircraft operation on sea ice (McMurdo).

It is well known that ice has two modes of response, elastic and inelastic, and that for each, the effects of temperature, salinity, thermal history, and load history are important parameters in the failure criterion. Unknowns in the constitutive equation for both linear (primary) and non-linear (secondary) creep of an ice plate, coupled with inadequate theory describing inelastic behavior of a plate supported by an elastic foundation, preclude establishing operating criteria by analytical techniques for the inelastic mode of response. Thus, the historical record of previous operations remains the principal source of information for evaluating long-term load effects.

As previously stated, this analysis is limited to the elastic mode of response to short-term loads associated with aircraft landings and takeoffs. Extension of the load time beyond 10 to 15 seconds, which is considered to be the time limit for purely elastic behavior of ice, introduces inelastic behavior and the gradual invalidating of a solution based on elastic theory.

Maximum movements and stresses, however, are developed during the elastic phase, which gradually relax with the inelastic behavior mode. Elastic analysis provides an estimate of the maximum stress imposed by loading, thus enabling an engineering prediction based on allowable stress below the failure stress or first-crack development. Operation of aircraft on sea ice is further safeguarded by the fact that in addition to criteria based on stress levels below failure stress, the floating ice sheet can accept loads beyond those causing the first crack. Formulas for estimating the collapse load were presented by Meyerhof.[5] His simplest formula for making a conservative estimate of the collapse load under short-term load conditions for a central load is:

$$P = \sigma h^2$$

where P = applied load (lb)

σ = flexural strength at failure (psi)

h = thickness of the ice sheet (in.)

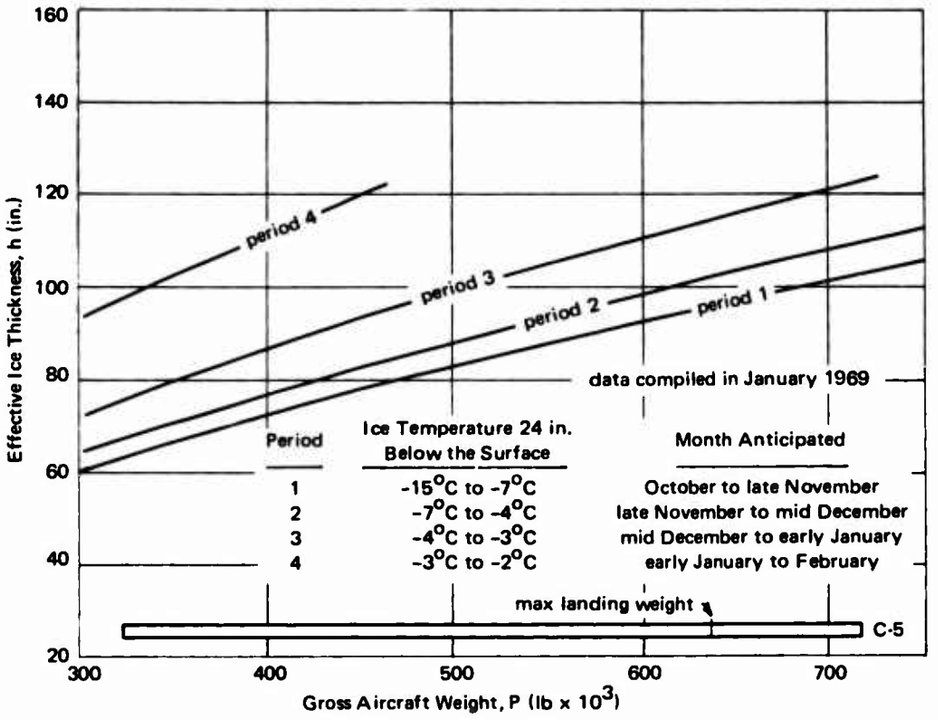

Figure 13. Load-versus-thickness requirements for C-5 aircraft operation on sea ice (McMurdo).

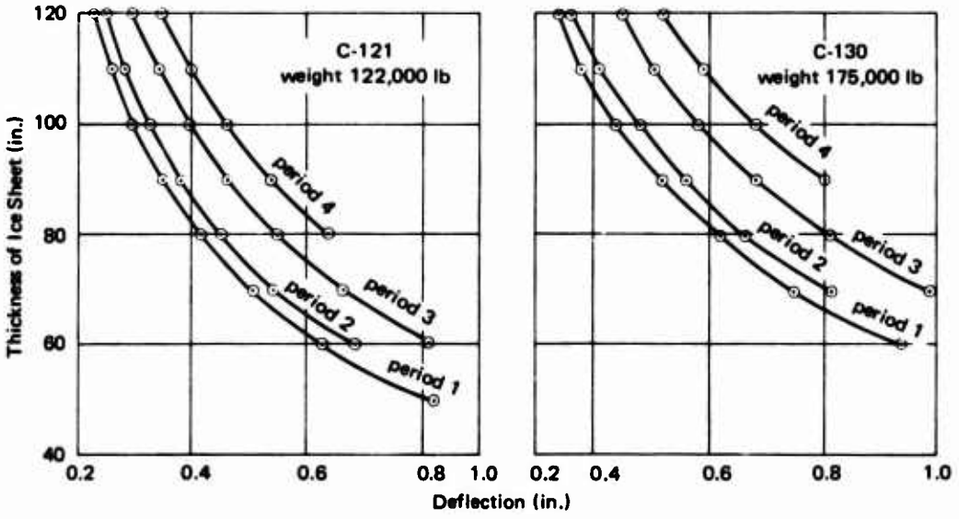

Figure 14. Elastic deflection of ice sheet based on maximum landing weights of C-121 and C-130 (calendar periods shown in Figure 3).

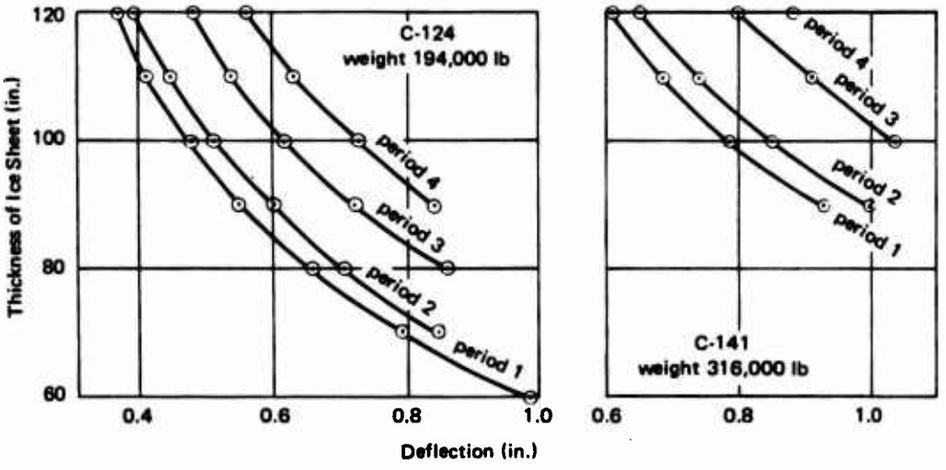

Figure 15. Elastic deflection of ice sheet based on maximum landing weights of C-124 and C-141 (calendar periods shown in Figure 3).

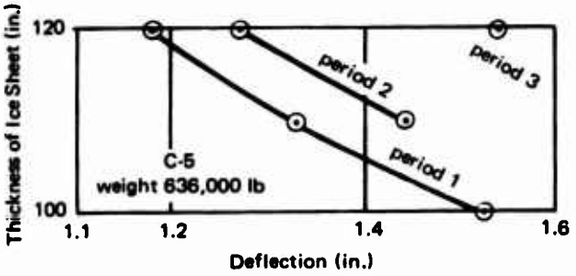

Figure 16. Elastic deflection of ice sheet based on maximum landing weight of C-5 (calendar periods shown in Figure 3).

The aircraft covered in this report comply with requirements of this formula, provided the area loaded by the aircraft is assumed to be a circle encompassing the main landing gear in order that the ratio of the load radius to the relative stiffness of the ice sheet be under 0.5. This assumption is reasonable when the spacing of the landing gear relative to the thickness of the ice plate is considered. In other words, a constant bending movement is assumed between the load points.

In the development of load curves, the normal idealization of elastic theory was assumed: (1) the relation between stress and strain is linear, (2) the principle of superposition holds, accordingly the summed stress and strain distribution from individual loads represents the effect of a combined load for small deflection, and (3) the ice sheet behaves as an isotropic media. The principle of superposition was used to accommodate the aircraft load distribution resulting from the landing gear configuration. The load from each landing gear strut was consequently treated as a uniformly loaded circular area, with one of the load areas in the gear configuration, for mathematical convenience, positioned over the zero coordinate of a rectangular coordinate system. The maximum confined load effect resulting from superimposing the effect of the other load areas was assumed to occur at the center of the zero coordinate load—it having been previously established that the maximum was at or very near the center location.

The mechanical properties of the ice used for the load-curve development were a combination of data derived from actual testing of the ice sheet at the McMurdo runway site and values selected from literature on reported testing of sea ice from arctic regions. The three mechanical properties involved in the solution are: (1) flexural strength, (2) elastic modulus, and (3) Poisson's ratio. The flexural strength, which has the predominant influence on the solution, was determined by in-situ testing of large beams cut from the local ice sheet. Beams were tested to provide flexural-strength data representative of the ice condition through the operating season. The literature values assigned for the elastic modulus were those determined by dynamic test methods with selection made on a temperature–salinity condition coinciding with those for the flexural-strength data. Poisson's ratio was treated as a constant function with a value of 0.3. The literature suggests it may vary from about 0.295 to about 0.333.

The load curves developed in this report provide operating criteria that are only moderately modified from those of the previous study;[1] they can therefore be confidently adopted to supersede the present operating criteria. These latest operating criteria benefit from a better understanding of the flexural-strength property of the ice sheet; this new knowledge permits a more finite association of the load capability of the ice sheet with its temperature. In addition, the solution is based entirely on elastic plate

theory, and this has eliminated the empirical method of "equivalent single-wheel load conversion" used in the previous solution. This change provides a more logical foundation for development of analytical methods for predicting the load-behavior characteristic of a floating ice sheet.

At the present, the lack of a good definition of all the failure mechanisms of an ice sheet precludes defining the safety factor provided by the solution. The environmental influence on the structural characteristics of the ice still requires on-the-spot interpretation. ***It is cautioned that this second generation of load curves presented in the report should not be used without the accompanying instructions (Appendix B) and, when necessary, modified by qualified on-the-spot evaluation of the site condition.*** Though the safety factor for the short-term load (elastic behavior mode) remains undefined, the solution is based on flexural-strength values which have been reduced by a factor ranging from 12% to 19% of the actual failure strength as determined from beam tests.

To determine the safety factor, one would have to establish that the mathematical theory accurately describes the structural behavior and defines what constitutes failure. For example, the elastic theory stops at the threshold of developing the first crack, but it is known from field experience that an ice sheet can be loaded considerably beyond this point before complete failure or collapse occurs. For the long-term load (inelastic behavior mode), a sensible failure criterion would be to establish a limit on sheet deflection.

CONCLUSIONS

1. The operating criteria developed in this study by utilizing standard elastic plate theory provide a better basis for future evaluation and refinement than the empirical approach developed in the previous study.[1]

2. The relation between flexural strength and temperature of the McMurdo ice sheet is better defined for this solution than for the previous solution.[1]

3. In the solution presented, the elastic modulus property has less direct influence on the load capacity of the ice than the flexural-strength property.

RECOMMENDATIONS

1. The mechanical properties of ice and the constitutive equations describing its behavior as a solid continuum should be more precisely defined. This includes:

a. Additional investigation into the flexural strength and elastic modulus as related to load rate, temperature, and salinity.

b. Investigation of primary and secondary creep properties for the development of constitutive equations to describe the inelastic behavior.

c. Investigation of load-distribution effect on stress and deformation for both elastic and inelastic modes of response.

2. Theories and/or solution methods that will adequately predict inelastic behavior of a plate supported on an elastic foundation should be developed.

3. The load curves developed in this report are recommended to replace present criteria for operating aircraft. They remain, however, only an interim solution to the determination of the bearing capacity of the McMurdo sea ice.

ACKNOWLEDGMENT

Mr. J. S. Hopkins contributed to the mathematical formulation of the problem and the computer programming. He is the author of Appendix A.

Appendix A

DEVELOPMENT OF ELASTIC THEORY ANALYSIS

by

J. S. Hopkins

MATHEMATICAL FORMULATION

The background for this program is provided by "Theory of Plates and Shells," by Timoshenko and Woinowsky-Krieger[4] (Chapter 1, Section 1; Chapter 2, Sections 9 through 11; Chapter 3, Section 15) and the abstract from "Deflections of an Infinite Plate," by Max Wyman.[5] The Timoshenko sections give basic plate theory, while the Wyman abstract gives stress and deflection formulas for a constant-density circular load on an infinite ice sheet supported by water.

In this program, which computes maximum aircraft load versus ice thickness for given maximum stress and elastic modulus, the aircraft landing gear is considered to be three or five circular plate loads, depending on the type of aircraft. For this reason, the program uses rectangular coordinates. The origin is as shown at the center of a main gear footprint. Differentiation of the functions was facilitated by their being polynomials in even powers of the radial distances from the centers of the circular gear footprints.

The landing gear load as shown in Figure A-1 has the origin of coordinates at 0. The landing gear prints are approximated as circles or disks for stress calculation. For some aircraft, such as the C-121, disks 3 and 4 would be missing. The stress per pound of load, **S**, is computed at 0, it having been established that 0 is at or very near to the maximum stress point for the configuration. The contributions from all the disks are superimposed at 0. After **S** has been computed, the maximum allowable aircraft weight, P_m, is computed from the given maximum stress σ_m, where $P_m = \sigma_m/S$. It has been found that the stress at 0 is at least 98.5% of the maximum stress. For the five aircraft types for which computations were made, the terminology used is listed below:

σ = stress (psi); σ_m = maximum allowable stress

S = stress per pound of aircraft load; i.e., $\sigma = SP$

a = radius (in.) of each disk, or landing gear print; same for all gear prints

P = gross aircraft landing weight (lb)

h = ice thickness (in.)

E = elastic modulus of ice (psi)

μ = Poisson's ratio, assumed constant at 0.3

PCMG = percentage of total aircraft load on each main gear

PCTW = percentage of total load on the nose gear

DH = distance (in.) between centers of disks 1 and 2, (also 3 and 4)

DV = distance (in.) between centers of disks 1 and 3 (also 2 and 4)

DTW = distance of nose gear from x axis (y coordinate of center of disk 5)

k = 0.037 lb/cu in., the density of water under the ice sheet; entirely analogous to the elastic constant of a solid supporting medium (comparing Pascal's law with Hooke's law).

r_i = $(x - a_i)^2 + (y - b_i)^2$ (going from rectangular to local polar coordinate); (a_i, b_i) denotes gear print center—i.e., for disk 2, (a_i, b_i) would be (**DH**, 0); r_i gives the distance out from the center of the disk.

From the above given quantities:

$$D = \frac{E h^3}{12(1 - \mu^2)} = \frac{E h^3}{10.92} = \text{flexural rigidity of plate} \qquad \text{(A-1)}$$

$$\ell = \sqrt{\frac{D}{k}} = \sqrt{\frac{D}{0.037}} = \text{radius of relative stiffness} \qquad \text{(A-2)}$$

$$BMG = \sqrt{1.6a^2 + h^2} - 0.675h \qquad \text{(A-3)}$$

$$b = \frac{BMG}{\ell} \qquad \text{(A-4)}$$

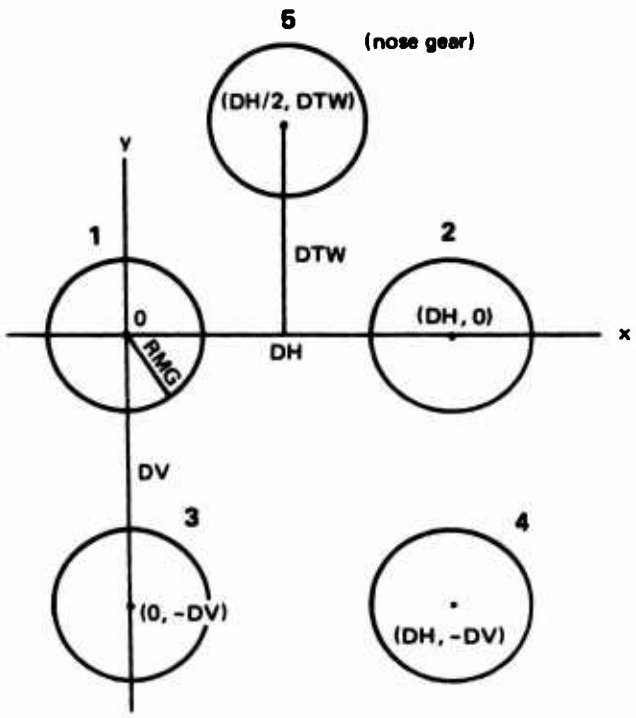

Figure A-1. Rectangular coordinates and landing gear positions.

Equation A-3 accounts for stress distribution effect as related to ice-sheet thickness (dependent on ratio of radius of load circle to plate thickness).

First computed is the stress/load contribution at 0 from wheel 1, centered at 0. Omitting **P** from Wyman's Equation 5.2, the result is:

$$S_o = \frac{3(1+\mu)\,PCMG\;kei'\,b}{\pi\,b\,h^2} = \frac{3.9\,PCMG\;kei'\,b}{\pi\,b\,h^2} \qquad \text{(A-5)}$$

For the contributions at point 0 of the other landing gear, the following formulas were used where subscript **i** denotes a single landing gear, and the sums (8b) are for all landing gear other than wheel 1.

Following Timoshenko and Wyman, where **w** denotes deflection of the ice sheet, and M_x and M_y are bending moments:

$$v_i = C1\;ker\,R_i - C2\;kei\,R_i \qquad \text{(A-6)}$$

$$\frac{\partial^2 v_i}{\partial x^2} = A1\,\frac{\partial^2}{\partial \epsilon^2}\,ker\,R_i - A2\,\frac{\partial^2}{\partial \epsilon^2}\,kei\,R_i \qquad \text{(A-7)}$$

where $v_i = w_i/P$

$\epsilon = x/\ell$

$R_i = r_i/\ell$

$C1 = (PCMG/0.037\,\pi\,b)\,ber'\,b$

$C2 = (PCMG/0.037\,\pi\,b)\,bei'\,b$

$A1 = C1/\ell^2$

$A2 = C2/\ell^2$ (A-8a)

Formulas for $\partial^2 v_i/\partial y^2$ are similar, also for $\partial^2 v_i/\partial x\,\partial y$.

For the nosewheel, **PCTW** replaces **PCMG**, and **T1**, **T2**, **B1**, **B2** are used instead of **S1**, **S2**, **A1**, **A2**.

$$\frac{\partial^2 v}{\partial x^2} = \sum_i \frac{\partial^2 v_i}{\partial x^2}$$

$$\frac{\partial^2 v}{\partial y^2} = \sum_i \frac{\partial^2 v_i}{\partial y^2} \qquad \text{(A-8b)}$$

$$\frac{\partial^2 v}{\partial x\,\partial y} = \sum_i \frac{\partial^2 v_i}{\partial x\,\partial y}$$

To obtain the principal directions of greatest and least curvature at point 0, Timoshenko's Equation 35 is used:

$$\alpha_1 = 0.5 \arctan\left(\frac{2\,\frac{\partial^2 v}{\partial x\,\partial y}}{\frac{\partial^2 v}{\partial x^2} - \frac{\partial^2 v}{\partial y^2}}\right) \qquad \text{(A-9)}$$

$$\alpha_2 = \alpha_1 + \frac{\pi}{2}$$

Generalizing Timoshenko's Equations 37 and 38 results in:

$$\left.\begin{aligned} m_n &= -D\left(\frac{\partial^2 v}{\partial n^2} + 0.3\,\frac{\partial^2 v}{\partial t^2}\right) \\ m_t &= -D\left(\frac{\partial^2 v}{\partial t^2} + 0.3\,\frac{\partial^2 v}{\partial n^2}\right) \end{aligned}\right\} \qquad \text{(A-10)}$$

where **n**, **t** are the directions of angles α_1, α_2, respectively, with respect to the x axis. Again the load, **P**, (which Wyman carries) is omitted as a factor, so that m_n and M_n are related by $M_n = P\,m_n$.

Computing directional derivatives and using Equation 10 results in:

$$m_n = -D\left[(\cos^2\alpha + 0.3\sin^2\alpha)\,\frac{\partial^2 v}{\partial x^2} + (\sin^2\alpha + 0.3\cos^2\alpha)\,\frac{\partial^2 v}{\partial y^2} + 0.7\,\frac{\partial^2 v}{\partial x\,\partial y}\right] \qquad \text{(A-11)}$$

$$m_t = -D\left[(\sin^2\alpha + 0.3\cos^2\alpha)\,\frac{\partial^2 v}{\partial x^2} + (\cos^2\alpha + 0.3\sin^2\alpha)\,\frac{\partial^2 v}{\partial y^2} - 0.7\,\frac{\partial^2 v}{\partial x\,\partial y}\right]$$

From Timoshenko's Equation 44, where the moment-to-stress constant is $6/h^2$, and continuing to omit load, **P**, as a factor, the resulting equation is:

$$\left.\begin{aligned} S_1 &= \frac{6\,m_n}{h^2} + S_o \\ S_2 &= \frac{6\,m_t}{h^2} + S_o \end{aligned}\right\} \qquad \text{(A-12)}$$

where S_o is the component of wheel 1 centered at 0, previously obtained in Equation A-5, letting: $S = \max(S_1, S_2)$.

Then, for a given maximum stress, σ_m, the maximum load is computed by:

$$P_m = \frac{\sigma_m}{S} \qquad \text{(A-13)}$$

For calculating the total deflection, let $v = v_o + \sum_i v_i$. If P_a = landing weight of the aircraft, given, then

$$P = \min(P_m, P_a) \tag{A-14}$$

The final deflection at 0 is

$$w = Pv \tag{A-15}$$

DIFFERENTIATION FORMULAS

In the following, a circular plate is considered centered at **a** and **b**. Since the **ker** and **kei** functions have argument r/ℓ, everything is normalized by dividing by ℓ to obtain:

$$R2 = \frac{(x-a)^2 + (y-b)^2}{\ell^2}$$

$$G = \gamma + 0.5 \ln(0.25\, R2)$$

where $\gamma = 0.5772$ (Euler's constant). Then

$$\left.\begin{aligned} &\frac{\partial R2}{\partial x} = \frac{2(x-a)}{\ell^2}, \quad \frac{\partial^2 R2}{\partial x} = \frac{2}{\ell^2}, \quad \frac{\partial^2 R2}{\partial x\, \partial y} = 0 \\ &\frac{\partial G}{\partial x} = \frac{x-a}{R2}, \quad \frac{\partial G}{\partial y} = \frac{y-b}{R2}, \quad \frac{\partial^2 G}{\partial x^2} = \frac{(y-b)^2 - (x-a)^2}{R2^2} \\ &\frac{\partial^2 G}{\partial y^2} = -\frac{\partial^2 G}{\partial x^2}, \quad \frac{\partial^2 G}{\partial x\, \partial y} = -\frac{2(x-a)(y-b)}{R2^2} \end{aligned}\right\} \tag{A-18}$$

With these aids, the following approximating polynomials and their derivatives can be written. The $1/\ell^2$ factor was absorbed into the constants A_1 and A_2 and will thus be omitted here.

$$\ker \frac{r}{\ell} = -G + \frac{\pi R2}{16} + \frac{(2G-3)R2^2}{128} - \frac{\pi R2^3}{9{,}216} + \frac{(25-12G)R2^4}{1{,}769{,}472} \tag{A-19}$$

$$\frac{\partial^2 \mathrm{ker}\ \frac{r}{\ell}}{\partial v^2} = \frac{(x-a)^2 - (y-b)^2}{R2^2} + \frac{\pi}{8} + \frac{(x-a)^2(8G-5)}{64} + \frac{(y-b)^2}{64}$$

$$+ \frac{[24G - 36 - \pi(x-a)^2]\,R2}{384} + \frac{R2^2[(85-48G)(x-a)^2 - 96\pi]}{147{,}456}$$

$$+ \frac{R2^3(25-12G)}{221{,}184} \qquad \text{(A-20)}$$

$$\frac{\partial^2 \mathrm{ker}\ \frac{r}{\ell}}{\partial x\,\partial y} = (x-a)(y-b)\left[\frac{2}{R2^2} + \frac{(4G-3)}{32} - \frac{\pi R2}{384} + \frac{R2^2(43-24G)}{73{,}728}\right.$$

$$\left. + \frac{\pi R2^3}{737{,}280}\right] \qquad \text{(A-21)}$$

$$\mathrm{kei}\ \frac{r}{\ell} = -\frac{\pi}{4} + 0.25(1-G)R2 + \frac{\pi R2^2}{256} + \frac{(6G-11)R2^3}{13{,}824}$$

$$- \frac{\pi R2^4}{589{,}824} \qquad \text{(A-22)}$$

$$\frac{\partial^2 \mathrm{kei}\ \frac{r}{\ell}}{\partial x^2} = 0.5(1-G) - \frac{0.75(x-a)^2}{R2} - \frac{0.25(y-b)^2}{R2} + \frac{\pi(x-a)^2}{32}$$

$$+ \frac{R2[36\pi + (24G-33)(x-a)^2 + (y-b)^2]}{2{,}304}$$

$$+ \frac{R2^2[96G - 176 - 3\pi(x-a)^2]}{36{,}864} \qquad \text{(A-23)}$$

$$\frac{\partial^2 \mathrm{kei}\ \frac{r}{\ell}}{\partial x\,\partial y} = (x-a)(y-b)\left[\frac{\pi}{32} - \frac{1}{2R2} + \frac{R2(12G-17)}{1{,}152} - \frac{\pi R2^2}{12{,}288}\right.$$

$$\left. + \frac{R2^3(2.47-1.2G)}{221{,}184}\right] \qquad \text{(A-24)}$$

INPUT CARDS

The input data to the program is entered on punched cards of two types. As many cards of each type may be punched as necessary for entry of the desired data. The input cards are placed behind the main program deck.

Stress-Modulus Cards

A maximum of six (σ_m, **E**) pairs may be entered on a card (Figure A-2). Data are filled in from the left, and unused σ - **E** fields are left blank, on the right.

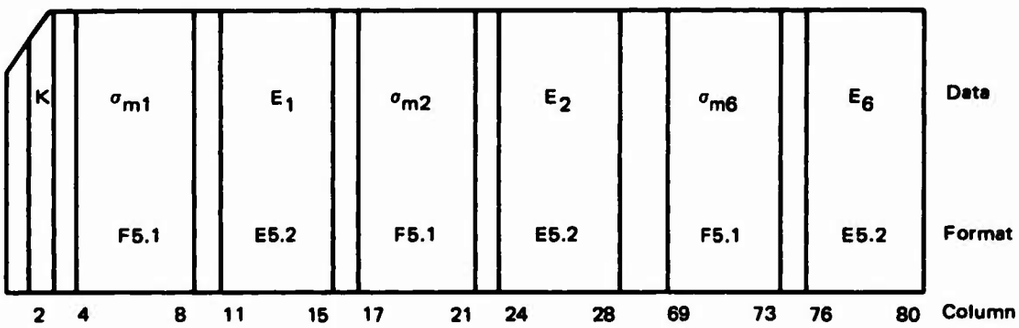

Figure A-2. Stress-modulus card format.

Aircraft Data Cards

One card (Figure A-3) is used for each type of aircraft. These are placed behind the stress-modulus card(s).

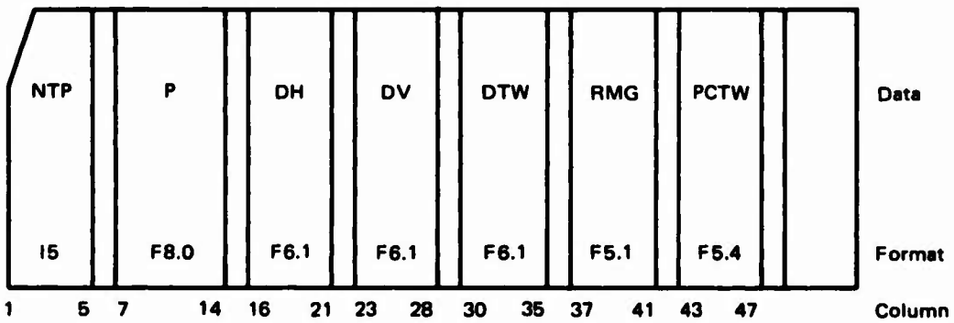

Figure A-3. Aircraft data card format.

Note: For **NTP** = 5, 121, 124, 130, or 141 (indicating aircraft C-5, etc.), only **NTP** and **P** need be punched. The other data, **DH**, etc., are internally stored for these aircraft.

K = blank or 0 if this is the last stress-modulus card.

= an integer 1 to 9 if more σ - **E** cards following.

σ_{mi} = maximum stress entry, psi. Examples are 29.1, 70.0, 126.3

E_i = elastic modulus entry paired with σ_{mi}. Examples are .42E6, .60E5. These entries represent 420,000 and 60,000.

NTP = aircraft type number. Right-justified in columns 1-5. Examples are 5, 12, 130. Letters are not included.

P = gross aircraft landing weight, lb. Example is 194,500., including decimal point.

DH, **DV**, **DTW**, **RMG** = gear-print spacing distances and radius (described in detail earlier), in inches. They are entered on the aircraft input cards under the same format. Examples are 1024.6, 324.0, 71.5. Entries not needed for aircraft types C-5, C-121, C-124, C-130, or C-141.

PCTW = percent of aircraft weight borne by the nosewheel. Examples are .0500, .1243. Not needed for aircraft types C-5, C-121, C-124, C-130, or C-141.

A program deck setup is illustrated in Figure A-4.

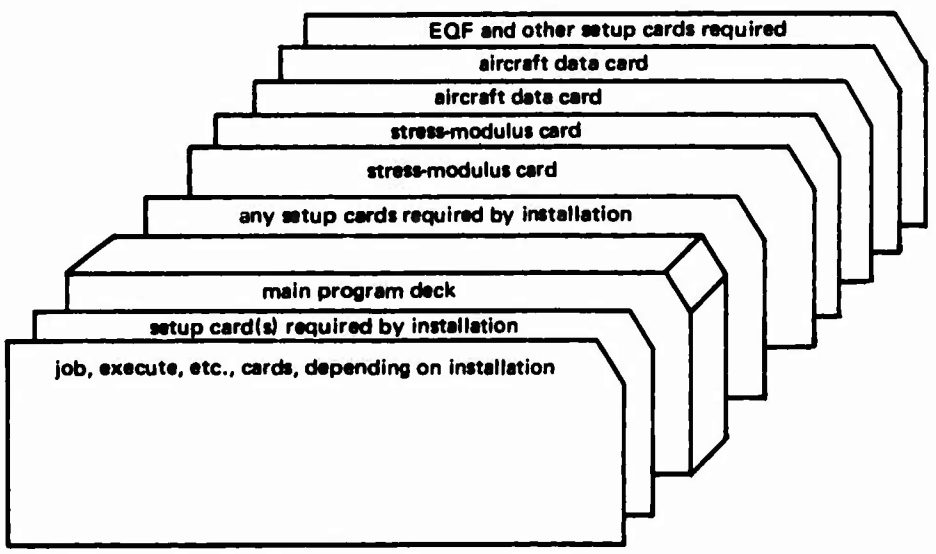

Figure A-4. Program deck setup.

Appendix B

LOAD CURVES FOR OPERATION OF AIRCRAFT ON SEA ICE AT MCMURDO, ANTARCTICA*

by

J. E. Dykins

LOAD CURVE DEVELOPMENT

The new load curves for operation of C-121, C-124, C-130, C-141, and C-5 aircraft on annual sea ice in the McMurdo area (Figures B-1 and B-2) are based on short-term loading of the ice sheet to near its elastic limit as determined by the elastic theory for plates. Figure B-1 provides the criteria for C-121, C-124, C-130, and C-141 aircraft, and Figure B-2 provides the criteria for the C-5 aircraft. The four load curves given in each of the figures represent the thickness-versus-load requirement for the operating season, October into February. Each of the curves is associated with the temperature of the ice sheet measured 24 inches below the surface; also included is the expected calendar occurrence of this temperature. At this depth, the ice sheet is fairly insensitive to daily temperature fluctuation; as a result, it is easy to associate the load curves with long-term warming or cooling (Figure B-3). The load curves were developed on the basis of the following allowable flexural stress in the ice:

Curve	Stress (psi)
1	80
2	70
3	55
4	35

The safety factor provided by these curves is not readily definable. The curves are based on elastic plate theory, which applies until the first crack is developed; however, for this solution, the maximum stresses that would be developed are conservative, well below those required to cause the initial crack. Additional safety is provided by the fact that an ice sheet

* These operating criteria are recommended to supersede the present criteria included in the Deep Freeze Operation Order Manual, first appearing in DF-68 manual.

can be loaded considerably beyond the point of developing the initial crack without complete failure. A conservative estimate of the failure load is obtained by the simple formula:

$$P = \sigma h^2$$

where P = weight of aircraft (lb)

σ = flexural strength of ice at failure (lb/in.^{2})

h = thickness of the ice sheet (in.)

As further evidence of adequate safety, the requirements of load versus thickness for the theoretical load curves are very close to the requirements of the empirical criteria for operating aircraft on ice sheets (NAVDOCKS DM-9, "Polar Engineering Design Manual"). There are, in addition, many documented cases of aircraft landing on and taking off from ice sheets of less thickness than specified by the load curves.

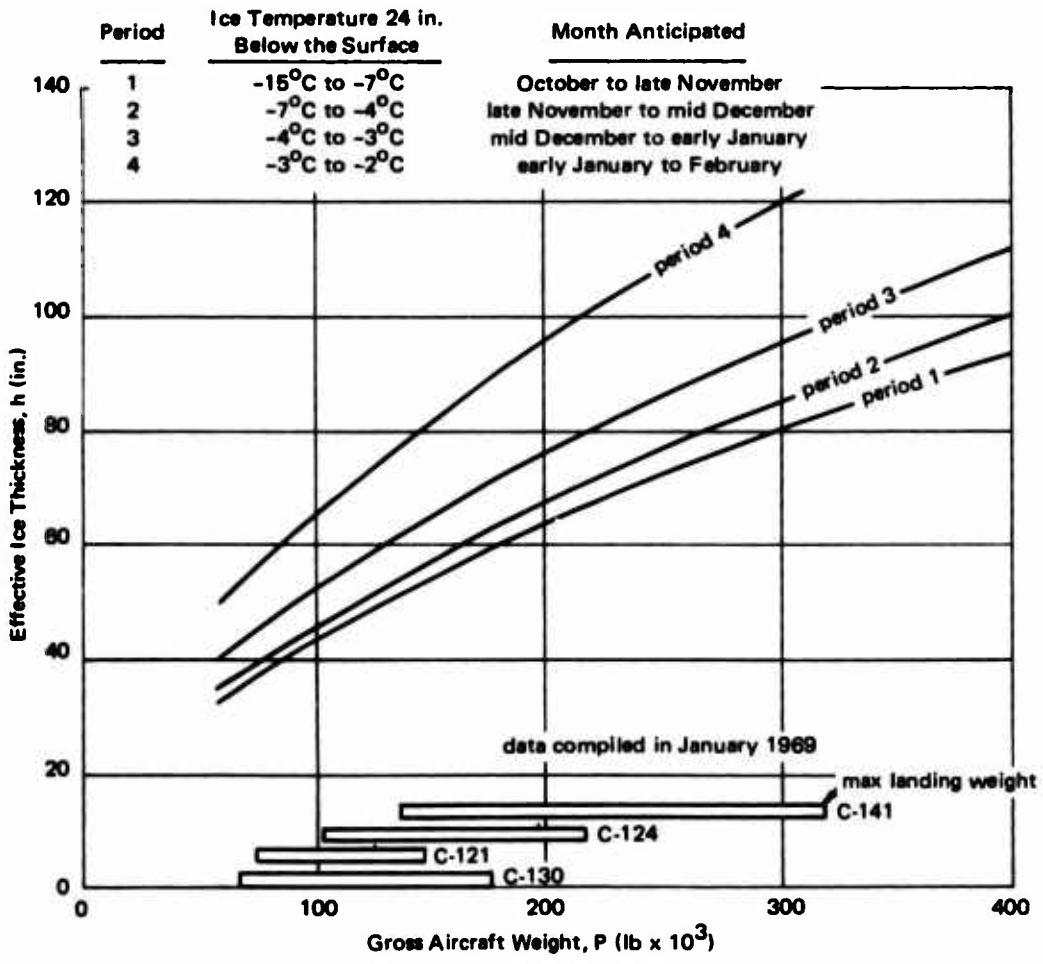

Figure B-1. Load-versus-thickness requirements for C-130, C-121, C-124, and C-141 aircraft operation on sea ice (McMurdo).

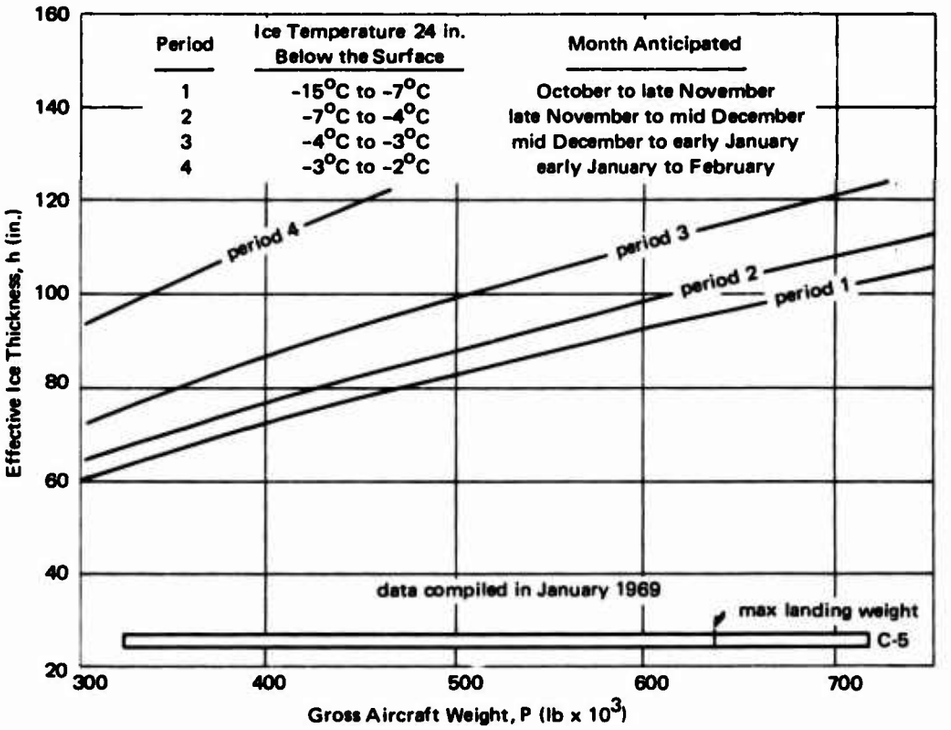

Figure B-2. Load-versus-thickness requirements for C-5 aircraft operation on sea ice (McMurdo).

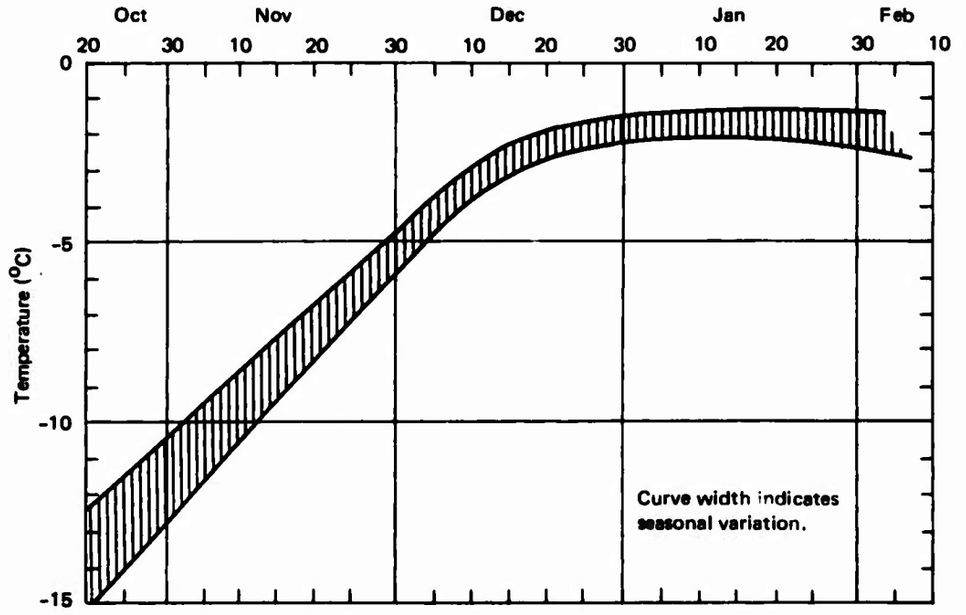

Figure B-3. Temperature of McMurdo annual sea ice at 24-inch depth.

The aircraft load curves have been developed on the basis of the favorable deep-water location and orientation of the present sea-ice runway, which minimizes the likelihood of stress reinforcements resulting from bottom or shoreline reflection.

Caution: Despite the safety factor provided in the operating criteria (load curves), on-the-spot evaluation and interpretation of the site condition is essential for the safety of aircraft and personnel.

FIELD PROCEDURE

The field procedure for operation of the C-121, C-124, C-130, C-141, and C-5 aircraft on the annual ice at McMurdo should be as follows.

Distance to Edge of Ice Sheet

No aircraft, whether landing, taxiing, taking off or standing (parked) should be closer than 500 feet to the edge of the ice sheet. Distances greater than this are preferred.

Ice-Thickness Surveys

The maintenance of a complete up-to-date ice-thickness survey for all aircraft operating areas is necessary for safe operation of the aircraft.

1. At the start of the operating season (October), a detailed thickness survey should be made down each edge of the sea-ice runway and around all other operating areas. Thickness stations on the runways should be at 500-foot intervals, with opposite stations staggered at midinterval.

2. During October and November, thickness measurements should be made at every other station at 10-day intervals to provide thickness information at 20-day intervals for each station. Field conditions may indicate a need for more frequent measurements.

3. Starting in December, the time interval between measurements should be decreased to 7 days, and by early January, daily measurements may be required if the ice conditions and aircraft operations warrant such surveillance.

4. Any soft, mushy-ice skeleton layer at the bottom of the sheet should be subtracted from the measured thickness to obtain the effective thickness of the ice for the curves in Figures B-1 and B-2. The thickness of this layer will vary considerably through the season. Until late December, this layer is normally new ice growth which has not completed solidification. By early January, the new growth should have disappeared; it may be replaced by a soft layer resulting from bottom deterioration. Because of this layer, the effective thickness of the ice is usually 2 to 6 inches less than the actual thickness. The thickness of the skeleton layer can only be determined by extracting cores from the ice with a 3-inch-diameter core auger.

5. Starting in late December, observation and inspection of the aircraft operating areas should be performed in great detail, particularly when the ice thickness versus aircraft weight coincides with or falls below the appropriate load curve (Figures B-1 and B-2).

Ice Temperatures

The maintenance of a complete up-to-date temperature record of the ice sheet at the 24-inch depth is necessary for use as a reference in determining which of the load curves (Figures B-1 and B-2) is in effect (a graphic plot of the daily temperature will simplify interpolation).

1. Permanent stations to measure temperatures with thermocouples or thermistors should be established at five or more locations dispersed for general coverage of the entire operational areas. Each permanent station should consist of two temperature probes, one 24 inches below the surface and one as a backup 20 inches below the surface. Normally, the daily 0800 temperature of the ice at the 24-inch level would be used to select the appropriate curve; however, if maintaining a daily record cannot be justified because of low aircraft use, the temperature should be taken more than once prior to use and preferably at an hour that is consistent with past records.

2. If permanent stations are not feasible, accurate mercury-bulb or dial thermometers should be used to measure the temperature at five or more locations in the aircraft operating areas. Each thermometer should be inserted into the ice in a newly drilled hole fitting the thermometer stem. Snow or chipped ice should be banked around the thermometer to reduce air effect on the temperatures. Also, the thermometers should be shielded from the direct rays of the sun. Measurements should be made as directed in the previous paragraph.

Ice-Runway Inspection

It is recommended that the entire runway be inspected after each landing and takeoff of aircraft when the aircraft weight and the effective ice thickness coincide with or fall below the in-effect load curves. A log should be maintained of cracks and other visual changes in the surface following such use. The development and spreading of cracks indicate that the runway has a near-capacity load, and further use should be suspended or continued on an emergency basis at reduced gross aircraft weights. This decision must be made in the field, as presently no numerical values can be assigned for this condition. The operational areas should be examined in great detail if noticeable sagging of the ice sheet is observed under the load.

Ice Creep Under Static Loads

Ice creeps under load; therefore, progressive deformation of the ice sheet can be expected under parked aircraft. The limit of permissible deformation has not been defined, but occurrence of one of the following two conditions will indicate an immediate need to move the aircraft:

(1) Deflection of the ice sheet to the extent that a circumferential crack starts to develop around the aircraft.

(2) Marked acceleration in rate of deflection.

It is recommended that any parked aircraft be moved when the deflection has reached 4 inches regardless of the nonoccurrence of either of the two warning conditions described above. A level or transit should be available at all times to measure the deflection at the aircraft when questionable conditions are evident. To determine this deflection, the instrument should be located at least 400 feet from the aircraft, and measurements near the main wheel of the aircraft should be compared with those 800 feet from the aircraft.

Aircraft Characteristics

The characteristics of the aircraft used for developing the curves in Figures B-1 and B-2 are shown in the body of the report as Figures 4 through 8.

REFERENCES

1. Naval Civil Engineering Laboratory. Technical Note N-888: Interim aircraft load curves for sea-ice runways at McMurdo, Antarctica, by J. E. Dykins. Port Hueneme, Calif., May 1967. (AD 815393L)

2. H. M. Westergaard. "Stresses in concrete pavements computed by theoretical analysis," Public Roads, vol. 7, no. 2, Apr. 1926, pp. 25-35.

3. S. Timoshenko and S. Woinowsky-Krieger. Theory of plates and shells, 2d ed. New York, McGraw-Hill, 1959, pp. 4-78.

4. M. Wyman. "Deflection of an infinite plate," Canadian Journal of Research, vol. 28, no. 3, sect. A, May 1950, pp. 293-302.

5. G. C. Meyerhof. "Bearing capacity of floating ice sheets," American Society of Civil Engineers, Transactions, vol. 127, pt. 1, 1962, pp. 524-581.

DISTRIBUTION LIST

SNDL Code	No. of Activities	Total Copies	
—	1	20	Defense Documentation Center
FKAIC	1	10	Naval Facilities Engineering Command
FKNI	13	13	NAVFAC Engineering Field Divisions
FKN5	9	9	Public Works Centers
FA25	1	1	Public Works Center
—	15	15	RDT&E Liaison Officers at NAVFAC Engineering Field Divisons and Construction Battalion Centers
—	183	183	NCEL Special Distribution List No. 7 for persons and activities interested in Polar Engineering

Unclassified

Security Classification

DOCUMENT CONTROL DATA - R & D

Security classification of title, body of abstract and indexing annotation must be entered when the overall report is classified)

1. ORIGINATING ACTIVITY (Corporate author) Naval Civil Engineering Laboratory Port Hueneme, California 93041	2a. REPORT SECURITY CLASSIFICATION Unclassified 2b. GROUP

3. REPORT TITLE

SEA-ICE BEARING STRENGTH IN ANTARCTICA—AIRCRAFT LOAD CURVES FOR MCMURDO ICE RUNWAY

4. DESCRIPTIVE NOTES (Type of report and inclusive dates)
Not final; June 1967—December 1968

5. AUTHOR(S) (First name, middle initial, last name)

J. E. Dykins

6. REPORT DATE September 1969	7a. TOTAL NO. OF PAGES 36	7b. NO. OF REFS 5
8a. CONTRACT OR GRANT NO b. PROJECT NO YF 38.536.002.01.001 c. d.	9a. ORIGINATOR'S REPORT NUMBER(S) TR-641 9b. OTHER REPORT NO(S) (Any other numbers that may be assigned this report)	

10. DISTRIBUTION STATEMENT

This document has been approved for public release and sale; its distribution is unlimited.

11. SUPPLEMENTARY NOTES	12. SPONSORING MILITARY ACTIVITY Naval Facilities Engineering Command Washington, D. C.

13. ABSTRACT

To update the operating criteria for C-121, C-124, C-130, C-141, and C-5 aircraft in the Antarctic, the bearing capacity of the McMurdo annual sea-ice sheet was analyzed for short-term loading. The load curves developed by elastic theory predict the ice thickness required as related to the changing strength characteristic of the ice sheet associated with the seasonal warming trend. These load curves provide operating criteria that are more related to the ice-sheet temperature than the operating criteria now in use. This analysis is only an interim solution in the development of aircraft operating criteria; continued research is needed to provide a better understanding of the ice-sheet response to both short- and long-term loads. The load curves and instructions presented in Appendix B are recommended to replace the present operating criteria appearing in NCEL Technical Note N-888, "Interim Aircraft Load Curves for Sea-Ice Runways at McMurdo, Antarctica."

DD FORM 1 NOV 65 1473 (PAGE 1)

S/N 0101-807-6801

Unclassified

Security Classification

14 KEY WORDS	LINK A		LINK B		LINK C	
	ROLE	WT	ROLE	WT	ROLE	WT
Sea-ice runways						
Antarctic						
Bearing strength						
Aircraft load curves						
Short-term loading						
Flexural strength						
Elastic behavior						